J. Fluid Mech. (1972), *vol.* 56, *part* 4, *pp.* 721–740
Printed in Great Britain

A general method for solving steady-state internal gravity wave problems

By D. G. HURLEY
Department of Mathematics, University of Western Australia

(Received 25 April 1972)

The paper describes a simple but general method for solving 'steady-state' problems involving internal gravity waves in a stably stratified liquid. Under the assumption that the motion is two-dimensional and that the Brunt–Väisälä frequency is constant, the method is used to re-derive in a very simple way the solutions to problems where the boundary of the liquid is either a wedge or a circular cylinder. The method is then used to investigate the effect that a model of the continental shelf has on an incident train of internal gravity waves. The method involves analytic continuation in the frequency of the disturbance, and may well prove to be effective for other types of wave problem.

1. Introduction and summary

The paper describes a simple but general method for solving steady-state problems involving internal gravity waves in a stably stratified liquid. It will be assumed that the motion is two-dimensional, and that the Brunt–Väisälä frequency N of the stratified liquid is constant, but neither of these assumptions is necessary for the success of the method.

Consider a line source of waves having the time variation $\exp\{-i\omega t\}$ in a stratified liquid that is bounded by certain rigid surfaces, some of which may extend to infinity. The resulting waves will be internal gravity ones if $\omega < N$; and we wish to derive the steady-state solution for this case. The problem is complicated by the necessity of satisfying the Sommerfeld radiation condition, and, unless the boundaries are very simple, its formulation involves a number of coupled integral equations (Robinson 1970*a*, *b*; Baines 1971*a*, *b*). However, the problem is considerably simpler when $\omega > N$, and here this case is considered first. The field equation is then elliptic, and a simple transformation in conjunction with the powerful method of conformal representation may be used to derive the solution that satisfies the Sommerfeld radiation condition for many different sorts of boundaries. This solution will be an analytic function of $\omega + i\epsilon$, where ϵ is a small positive number, so that analytic continuation may be used to obtain the solution when $\omega < N$. Knowing the solution for a source, we may use distributions of sources to solve problems in which there is an incident wave and/or a prescribed motion of the boundaries.

The plan of the paper is as follows. Section 2 gives the basic equations, and the general procedure for determining the Green's function. Section 3 gives details of the Green's function for a wedge of stratified liquid. Only minor changes in the

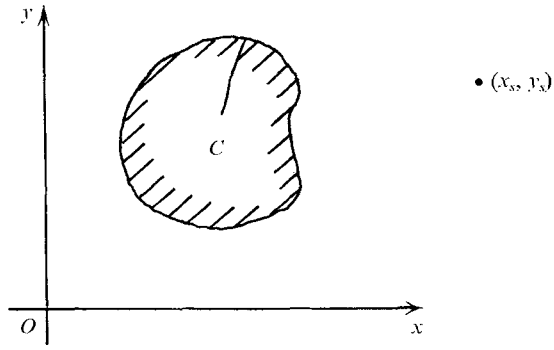

FIGURE 1. Notation.

method are needed to obtain the eigenfunctions instead of the Green's function, and this is illustrated in §4 for the case of a circular cylinder. Section 5 describes an investigation of the effect that a model of the continental shelf has on an incident train of internal gravity waves.

2. A general method for determining the Green's function

We consider the two-dimensional motion of an inviscid, stably stratified liquid whose Brunt–Väisälä frequency N is constant, and take Cartesian axes Oxy in the plane of the motion, where Ox is horizontal and Oy is vertical. We suppose that the liquid is bounded internally by a solid cylinder whose trace in the Oxy plane is the closed curve C, and that there is a line source of strength $\exp\{-i\omega t\}$ at the point (x_s, y_s) which is outside C (see figure 1). A stream function

$$\hat{\psi} = \psi(x, y; \omega) \exp\{-i\omega t\} \tag{2.1}$$

(which we shall refer to as the Green's function) exists, in terms of which the velocity components (u, v) are given by

$$u = -\frac{\partial \hat{\psi}}{\partial y}, \quad v = \frac{\partial \hat{\psi}}{\partial x}. \tag{2.2}$$

When $\omega < N$, the waves that occur will be internal gravity ones, and ψ will satisfy the hyperbolic equation

$$\frac{\partial^2 \psi}{\partial y^2} - \eta^2 \frac{\partial^2 \psi}{\partial x^2} = 0, \tag{2.3}$$

where

$$\eta^2 = \frac{N^2}{\omega^2} - 1, \tag{2.4}$$

and the boundary conditions,

$$\psi = 0 \text{ on } C, \tag{2.5}$$

and

$$\psi \sim -\frac{i}{4\pi} \log\left\{\frac{\sigma_- - \sigma_{-s}}{\sigma_+ - \sigma_{+s}}\right\} \quad \text{near} \quad x_s, y_s, \tag{2.6}$$

where

$$\left.\begin{aligned} \sigma_- &= x \sin\mu + y \cos\mu, \\ \sigma_+ &= x \sin\mu - y \cos\mu, \end{aligned}\right\} \tag{2.7}$$

$$\mu = \cot^{-1}\eta \tag{2.8}$$

(Hurley 1969), and the subscripts s denote values at the source point. ψ must also satisfy the Sommerfeld radiation condition.

The required solution will be of the form

$$\psi = f(\sigma_+) + g(\sigma_-), \tag{2.9}$$

where f and g are complex-valued functions. The radiation condition may be satisfied by replacing ω in (2.1) and (2.4) by $\omega + i\epsilon$, $\epsilon > 0$, determining the required solution $\psi(x, y; \omega + i\epsilon)$, and then taking the limit $\epsilon \to 0$ of it. Physically this corresponds to allowing the motion to grow gradually from zero like $\exp\{\epsilon t\}$ (Lighthill 1966). To the first order in ϵ, (2.4) becomes

$$\eta^2 = \frac{N^2}{\omega^2} - 1 - \frac{2iN^2\epsilon}{\omega^3}, \tag{2.10}$$

and, if this expression is substituted into (2.3), it is found that both the real and the imaginary parts of ψ satisfy

$$\left\{\left(\frac{N^2}{\omega^2} - 1\right)^2 + \frac{4N^4\epsilon^2}{\omega^6}\right\}\frac{\partial^4 h}{\partial x^4} - 2\left(\frac{N^2}{\omega^2} - 1\right)\frac{\partial^4 h}{\partial x^2 \partial y^2} + \frac{\partial^4 h}{\partial y^4} = 0. \tag{2.11}$$

Now (2.11) is elliptic for all real values of ω, so that its solution $\psi(x, y; \omega + i\epsilon)$ will be analytic in x and y (see e.g. Bers, John & Schechter 1964, p. 136). Thus, in particular, analytic continuation in x and y (with ϵ in (2.10) $\neq 0$) may be used to determine those branches of the logarithms in (2.6) that are appropriate to the various regions of the Oxy plane. Also, $\psi(x, y; \omega)$, being the response of the system to a disturbance having frequency ω, has the nature of a Fourier transform, and may therefore be expected to be an analytic function of the complex variable $\omega + i\epsilon$ (see e.g. Carrier, Krook & Pearson 1966, p. 301). However, a rigorous proof that this is so in the general case is not needed, because, for any particular problem, we shall determine $\psi(x, y; \omega + i\epsilon)$ explicitly, and its analyticity in $\omega + i\epsilon$ will be apparent. Thus, in particular, it is clear that analytic continuation in ω may be used to derive the solution of (2.11) for the case $\omega > N$ from the solution for the case $\omega < N$, and conversely.

Now, if we replace ω by $\omega + i\epsilon$ in (2.3)–(2.9), let ω take values greater than N and then take the limit $\epsilon \to 0$, we obtain the following results:

$$\eta = \left(\frac{N^2}{\omega^2} - 1\right)^{\frac{1}{2}} \text{becomes } -i\alpha \text{ where } \alpha^2 = 1 - \frac{N^2}{\omega^2}, \tag{2.12}$$

$$\sigma_- \text{ becomes } \frac{\omega}{N}(x - i\alpha y), \quad \sigma_+ \text{ becomes } \frac{\omega}{N}(x + i\alpha y), \tag{2.13}$$

$$(2.3) \text{ becomes } \frac{\partial^2 \psi}{\partial y^2} + \alpha^2 \frac{\partial^2 \psi}{\partial x^2} = 0, \tag{2.14}$$

and

$$(2.6) \text{ becomes } \psi \sim -\frac{1}{2\pi}\tan^{-1}\left\{\frac{\alpha(y - y_s)}{x - x_s}\right\} \text{ near } x_s, y_s. \tag{2.15}$$

Finally

$$(2.9) \text{ becomes } \psi = f^*\left(\frac{x + i\alpha y}{(1 - \alpha^2)^{\frac{1}{2}}}\right) + g^*\left(\frac{x - i\alpha y}{(1 - \pi\alpha^2)^{\frac{1}{2}}}\right), \tag{2.16}$$

where f^* and g^* are the functions of the arguments shown that result from the analytic continuation of (2.9). In general, f^* will not be the same function as f, and g^* will not be the same function as g.

Putting

$$x' = x/\alpha, \quad y' = y \tag{2.17}$$

transforms (2.14), (2.15) and (2.5) to

$$\frac{\partial^2 \psi}{\partial y'^2} + \frac{\partial^2 \psi}{\partial x'^2} = 0, \tag{2.18}$$

$$\psi \sim -\frac{1}{2\pi} \tan^{-1}\left\{\frac{y'-y'_s}{x'-x'_s}\right\} \text{ near } x'_s, y'_s, \tag{2.19}$$

and

$$\psi = 0 \quad \text{on} \quad C' \tag{2.20}$$

respectively, where C' is the curve in the $Ox'y'$ plane into which the curve C maps under the transformation (2.17).

The problem of determining ψ so that it satisfies (2.18)–(2.20) is simply that of determining the potential flow due to a unit line source at (x'_s, y'_s) in the presence of the solid boundary C', and may be carried out in many cases by using conformal representation. Let the complex velocity potential of the motion in the x', y' plane be $w(x'+iy')$, so that (Milne-Thomson 1949, §5.14)

$$\psi = -\frac{i}{2}\{w(x'+iy') - \overline{w}(x'-iy')\} \tag{2.21}$$

$$= -\frac{i}{2}\left\{w\left(\frac{x+i\alpha y}{\alpha}\right) - \overline{w}\left(\frac{x-i\alpha y}{\alpha}\right)\right\}, \tag{2.22}$$

using (2.17).

Since for a given w there is a unique way of expressing ψ in the form (2.21), a comparison of (2.22) with (2.16) shows that we have succeeded in determining f^* and g^* uniquely.

Hence, to obtain the solution to the boundary-value problem posed by (2.3)–(2.8), we have merely to obtain the solution (2.21) to a simple potential flow problem, and then carry out in reverse the analytic continuation procedure described above, to obtain the desired solution (2.9). The radiation condition will be satisfied if the branches of the many-valued functions f and g are determined by replacing ω by $\omega + i\epsilon$, carrying out analytic continuation in x and y and then taking the limit $\epsilon \to 0$. We illustrate the method by considering the following examples.

3. Source in a wedge

Consider a source in the wedge of stratified liquid shown in figure 2. The face OA of the wedge coincides with the Ox axis and the face OB is inclined at an angle θ_B to it. θ_B may have any value between O and 2π.

As explained in §2, we first consider the case when $\omega > N$. The transformation (2.17) maps the wedge in the Oxy plane into one in the $Ox'y'$ plane having an angle of

$$\theta'_B = \tan^{-1}(\alpha \tan \theta_B), \tag{3.1}$$

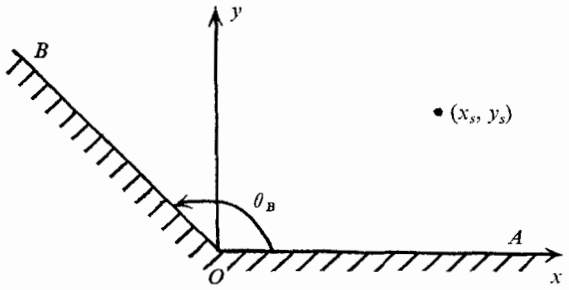

FIGURE 2. Source in wedge of stratified liquid.

and maps the source point to the point.

$$x' = x_s/\alpha, \quad y' = y_s. \tag{3.2}$$

By mapping the wedge-shaped region of the Z' $(= x' + iy')$ plane onto the upper half of the Z'' plane by means of the transformation

$$Z'' = Z'^{\pi/\theta'_B}, \tag{3.3}$$

we find that the complex velocity potential of the motion due to a unit source at the point $(x_s/\alpha, y_s)$ in the Z' plane is

$$w = -\frac{1}{2\pi}\log\{(Z''-Z''_s)(Z''-\bar{Z}''_s)\}, \tag{3.4}$$

where the overbar denotes complex conjugate. Equations (2.21), (3.3) and (3.4) give

$$\psi = \frac{i}{4\pi}\log\left[\frac{(Z'^{\pi/\theta'_B}-Z_s'^{\pi/\theta'_B})(Z_s'^{\pi/\theta'_B}-\bar{Z}_s'^{\pi/\theta'_B})}{(\bar{Z}'^{\pi/\theta'_B}-\bar{Z}_s'^{\pi/\theta'_B})(\bar{Z}'^{\pi/\theta'_B}-Z_s'^{\pi/\theta'_B})}\right]. \tag{3.5}$$

Equations (3.5), (3.1) and (2.17) give ψ in terms of x, y and θ_B for the case $\omega > N$.

Equations (2.13), (2.17) and (3.1) show that, to carry out the analytic continuation to determine the solution when $\omega < N$, we replace

$$\left.\begin{aligned} \frac{\alpha Z'}{(1-\alpha^2)^{\frac{1}{2}}} \quad &\text{by} \quad \sigma_+, \\ \frac{\alpha \bar{Z}'}{(1-\alpha^2)^{\frac{1}{2}}} \quad &\text{by} \quad \sigma_-, \end{aligned}\right\} \tag{3.6}$$

and

$$\pi/\theta'_B \quad \text{by} \quad -2\pi i/C, \tag{3.7}$$

where

$$C = \log\left(\frac{x_B-\eta y_B}{x_B+\eta y_B}\right), \tag{3.8}$$

and the subscript B denotes values at any point on the face OB of the wedge (see figure 2). Hence

$$\psi = \frac{-i}{4\pi}\log\left\{\frac{(1-\exp\{-i\alpha_1\})(1-\exp\{-i\alpha_3\})}{(1-\exp\{-i\alpha_2\})(1-\exp\{-i\alpha_4\})}\right\}, \tag{3.9}$$

where

$$\left.\begin{aligned} \alpha_1 = \frac{2\pi}{C}\log\left(\frac{x+\eta y}{x_s+\eta y_s}\right), \quad \alpha_2 = \frac{2\pi}{C}\log\left(\frac{x-\eta y}{x_s-\eta y_s}\right), \\ \alpha_3 = \frac{2\pi}{C}\log\left(\frac{x+\eta y}{x_s-\eta y_s}\right), \quad \alpha_4 = \frac{2\pi}{C}\log\left(\frac{x-\eta y}{x_s+\eta y_s}\right). \end{aligned}\right\} \tag{3.10}$$

Equation (3.9) agrees with Hurley (1970, (3.11)) if a minor error in the latter is corrected: the 8 in the denominator should be replaced by a 4. This error does not affect the subsequent analysis described therein.

4. Eigenfunctions for a circular cylinder

Consider a circular cylinder of radius a, whose surface is executing small oscillations with time variation $\exp\{-i\omega t\}$. The stream function for the motion outside the cylinder will be of the form (2.1), and must satisfy the radiation condition and also the boundary condition

$$\psi = F(\theta) \quad \text{on} \quad x = a\cos\theta, \quad y = a\sin\theta, \tag{4.1}$$

where F is some function that depends on the nature of the oscillations.

When $\omega > N$, (2.17) maps the circle $x^2+y^2 = a^2$ into an ellipse in the Z' plane, and, by using the Joukowski transformation

$$Z'' = \frac{1}{2}\left\{Z' + \left[Z'^2 - \frac{a^2(1-\alpha^2)}{\alpha^2}\right]^{\frac{1}{2}}\right\}, \tag{4.2}$$

it may readily be shown that the most general form for ψ, that represents motions in which the fluid velocities decay at large distances, is

$$\psi = a_0 \log Z'' + \sum_{n=1}^{\infty} a_n Z''^{-n} + \bar{a}_0 \log \bar{Z}'' + \sum_{n=1}^{\infty} \bar{a}_n \bar{Z}''^{-n}. \tag{4.3}$$

Using the results of §2, it is found that the analytic continuation of (4.3) for $\omega < N$ is

$$\begin{aligned}\psi = {} & C_0 \log\left(\frac{\sigma_+}{a} + \left[\frac{\sigma_+^2}{a^2} - 1\right]^{\frac{1}{2}}\right) + \sum_{n=1}^{\infty} c_n \left(\frac{\sigma_+}{a} + \left[\frac{\sigma_+^2}{a^2} - 1\right]^{\frac{1}{2}}\right)^{-n} \\ & + d_0 \log\left(\frac{\sigma_-}{a} + \left[\frac{\sigma_-^2}{a^2} - 1\right]^{\frac{1}{2}}\right) + \sum_{n=1}^{\infty} d_n \left(\frac{\sigma_-}{a} + \left[\frac{\sigma_-^2}{a^2} - 1\right]^{\frac{1}{2}}\right)^{-n},\end{aligned} \tag{4.4}$$

with $[\sigma_-^2/a^2 - 1]^{\frac{1}{2}}$ and $[\sigma_+^2/a^2 - 1]^{\frac{1}{2}}$ taking the values shown in figures 3 and 4.

The pressure p in the liquid may be obtained from the relations (see e.g. Hurley 1969)

$$\frac{\partial p}{\partial \sigma_+} = i\rho_0 \omega \eta \frac{\partial \psi}{\partial \sigma_+}, \quad \frac{\partial p}{\partial \sigma_-} = -i\rho_0 \omega \eta \frac{\partial \psi}{\partial \sigma_-}; \tag{4.5}$$

and the imposition of the condition

$$\oint_C p\, ds = 0 \tag{4.6}$$

(where C is any closed contour surrounding the cylinder) shows that c_0 and d_0 in (4.4) must satisfy the relation

$$c_0 + d_0 = 0. \tag{4.7}$$

Hence the most general form for the stream function is

$$\begin{aligned}\psi = {} & S_0 \log\left\{\frac{\sigma_+/a + [\sigma_+^2/a^2 - 1]^{\frac{1}{2}}}{\sigma_-/a + [\sigma_-^2/a^2 - 1]^{\frac{1}{2}}}\right\} + \sum_{n=1}^{\infty} c_n \left(\frac{\sigma_+}{a} + \left[\frac{\sigma_+^2}{a^2} - 1\right]^{\frac{1}{2}}\right)^{-n} \\ & + \sum_{n=1}^{\infty} d_n \left(\frac{\sigma_-}{a} + \left[\frac{\sigma_-^2}{a^2} - 1\right]^{\frac{1}{2}}\right)^{-n}.\end{aligned} \tag{4.8}$$

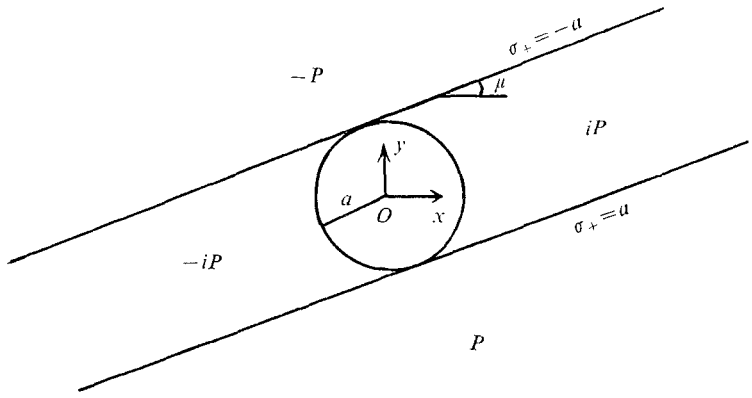

FIGURE 3. Values of $(\sigma_+^2/a^2-1)^{\frac{1}{2}}$ in $x^2+y^2 > a^2$.
P denotes the positive real number $|\sigma_+^2/a^2-1|^{\frac{1}{2}}$.

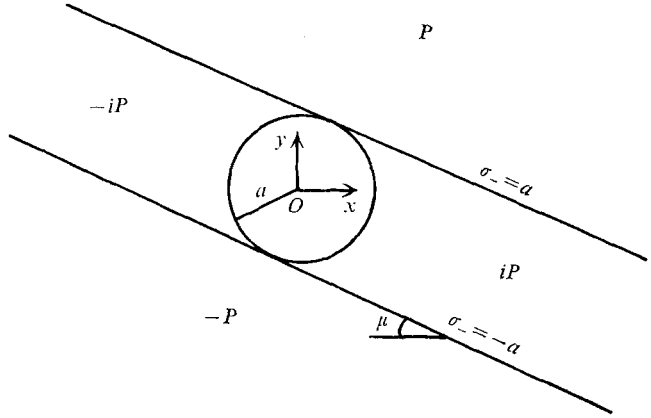

FIGURE 4. Values of $(\sigma_-^2/a^2-1)^{\frac{1}{2}}$ in $x^2+y^2 > a^2$.
P denotes the positive real number $|\sigma_-^2/a^2-1|^{\frac{1}{2}}$.

On the surface of the cylinder,

$$\frac{\sigma_-}{a}+\left[\frac{\sigma^2}{a^2}-1\right]^{\frac{1}{2}} = i\exp\{-i(\theta+\mu)\} \tag{4.9}$$

and

$$\frac{\sigma_+}{a}+\left[\frac{\sigma_+^2}{a^2}-1\right]^{\frac{1}{2}} = i\exp\{i(\theta-\mu)\},$$

so that the expansion (4.8) is complete and unique.

The terms in the infinite series in (4.8) have been used by Barcilon & Bleistein (1969*a*, *b*), but their determination of the square roots was incorrect and as a consequence the radiation condition was not satisfied (Baines 1971*a*).

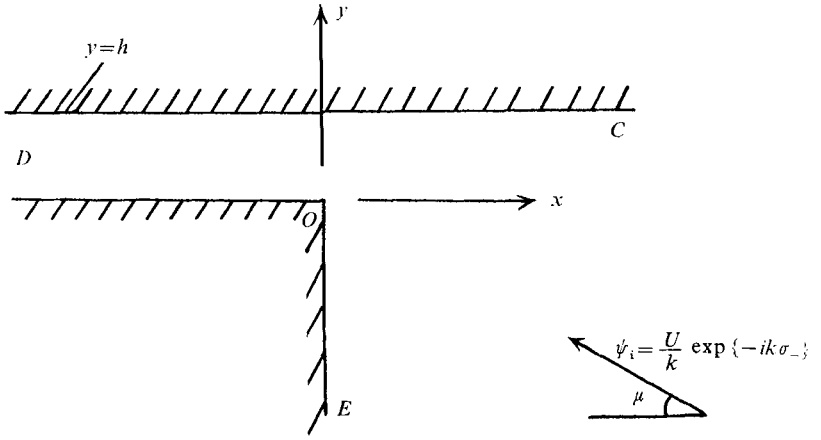

FIGURE 5. Model of continental shelf in $z = x + iy$ plane.

5. The effect of the continental shelf on a train of internal gravity waves

Suppose that the internal gravity wave

$$\psi_i = U/k \exp\{-ik\sigma_-\} \tag{5.1}$$

is incident on the model of the continental shelf shown in figure 5. Here the line $y = h$ represents the surface of the ocean, and the half lines $y = 0$, $x < 0$ and $x = 0$, $y < 0$ the continental shelf itself. On each of these lines the normal velocity must be zero (Phillips 1966, p. 165). The group velocity of the incident wave is in the direction of the arrow in the figure. Let

$$\psi = \psi_i + \psi', \tag{5.2}$$

so that ψ' is the disturbance stream function, which were present as a distribution of sources (Green's functions) along OE, OD and DC, of such a strength as to give zero total normal velocity thereon. Thus

$$\begin{aligned}\psi' = &-2iU\cos\mu\int_{-\infty}^{0}\exp\{-iky_s\cos\mu\}G_{OE}(x,y;y_s)\,dy_s\\ &+2iU\sin\mu\int_{-\infty}^{0}\exp\{-ikx_s\sin\mu\}G_{OD}(x,y;x_s)\,dx_s\\ &-2iU\sin\mu\int_{-\infty}^{\infty}\exp\{-ik(x_s\sin\mu+h\cos\mu)\}G_{DC}(x,y;x_s)\,dx_s,\end{aligned} \tag{5.3}$$

where G_{OE}, G_{OD} and G_{DC} are the Green's functions for sources of unit strength on OE, OD and DC, respectively, with each of these lines a streamline.

To determine the G's we first consider the case $\omega > N$. It follows from (2.17) that the boundaries in the Z and Z' planes are the same; and an application of the Schwartz–Christoffel theorem shows that the appropriate region of the Z' plane is mapped onto the upper half of the Z'' plane in the manner shown in figure 6, by the transformation

$$Z' = -\frac{2ih}{\pi}Z''^{\frac{1}{2}} + \frac{h}{\pi}\log\frac{1+iZ''^{\frac{1}{2}}}{1-iZ''^{\frac{1}{2}}}, \tag{5.4}$$

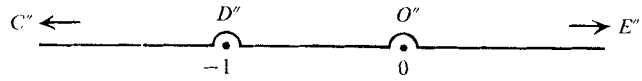

FIGURE 6. $Z'' = x'' + iy''$ plane.

where $Z''^{\frac{1}{2}}$ has its principal value and

$$\log \frac{1+iZ''^{\frac{1}{2}}}{1-iZ''^{\frac{1}{2}}} \to i\pi \quad \text{as} \quad Z'' \to +\infty.$$

For a unit source at the point that maps to Z''_s we have

$$w = -\frac{1}{2\pi}\{\log[(Z''-Z''_s)(Z''-\bar{Z}''_s)]\}. \tag{5.5}$$

$w(Z')$ is given implicitly by (5.4) and (5.5), $\overline{w}(\bar{Z}')$ by their complex conjugates and each of G_{OE}, G_{OD} and G_{DC} by the limit as Z_s approaches the appropriate boundary of

$$G = -\frac{i}{4}\{w(Z') - \overline{w}(\bar{Z}')\}. \tag{5.6}$$

For the case $\omega < N$, (2.13), (5.4) and (5.5) show that

$$w = -\frac{1}{2\pi}\log\{[Z''_+(\sigma_+) - Z''_+(\sigma_{+s})][Z''_+(\sigma_+) - Z''_-(\sigma_{-s})]\}, \tag{5.7}$$

$$\overline{w} = -\frac{1}{2\pi}\log\{[Z''_-(\sigma_-) - Z''_-(\sigma_{-s})][Z''_-(\sigma_-) - Z''_-(\sigma_{+s})]\}, \tag{5.8}$$

where the function $Z''_+(t)$ is defined implicitly by

$$\frac{(1+\eta^2)^{\frac{1}{2}}}{i\eta}t = \frac{-2ih}{\pi}Z''^{\frac{1}{2}}_+ + \frac{h}{\pi}\log\frac{1+iZ''^{\frac{1}{2}}_+}{1-iZ''^{\frac{1}{2}}_+} \tag{5.9}$$

and the function $Z''_-(t)$ by

$$\frac{(1+\eta^2)^{\frac{1}{2}}}{i\eta}t = \frac{2ih}{\pi}Z''^{\frac{1}{2}}_- - \frac{h}{\pi}\log\frac{1+iZ''^{\frac{1}{2}}_-}{1-iZ''^{\frac{1}{2}}_-}. \tag{5.10}$$

G is still given by (5.6). Hence

$$\psi' = \psi'_+(\sigma_+) + \psi'_-(\sigma_-), \tag{5.11}$$

where

$$\begin{aligned}\psi'_+(\sigma_+) = {} & \frac{U\cos\mu}{4\pi}\int_{-\infty}^{0}\exp\{-iky_s\cos\mu\}\log\{[Z''_+(\sigma_+) - Z''_+(-y_s\cos\mu)] \\ & \times [Z''_+(\sigma_+) - Z''_-(y_s\cos\mu)]\}\,dy_s \\ & - \frac{U\sin\mu}{4\pi}\int_{-\infty}^{0}\exp\{-ikx_s\sin\mu\}\log\{[Z''_+(\sigma_+) - Z''_+(x_s\sin\mu)] \\ & \times [Z''_+(\sigma_+) - Z''_-(x_s\sin\mu)]\}\,dx_s \\ & + \frac{U\sin\mu}{4\pi}\int_{-\infty}^{\infty}\exp\{-ik(x_s\sin\mu + h\cos\mu)\}\log\{[Z''_+(\sigma_+) - Z''_+(x_s\sin\mu - h\cos\mu)] \\ & \times [Z''_+(\sigma_+) - Z''_-(x_s\sin\mu + h\cos\mu)]\}\,dx_s, \end{aligned} \tag{5.12}$$

and

$$\psi'_-(\sigma_-) = -\frac{U\cos\mu}{4\pi}\int_{-\infty}^{0}\exp\{-iky_s\cos\mu\}\log\{[Z''_-(\sigma_-)-Z''_-(y_s\cos\mu)] \times[Z''_-(\sigma_-)-Z''_+(-y_s\cos\mu)]\}dy_s$$
$$+\frac{U\sin\mu}{4\pi}\int_{-\infty}^{0}\exp\{-ikx_s\sin\mu\}\log\{[Z''(\sigma_-)-Z''_-(x_s\sin\mu)] \times[Z''_-(\sigma_-)-[Z''_+(x_s\sin\mu)]\}dx_s$$
$$-\frac{U\sin\mu}{4\pi}\int_{-\infty}^{\infty}\exp\{-ik(x_s\sin\mu+h\cos\mu)\}\log\{(Z''_-(\sigma_-) - Z''_-(x_s\sin\mu+h\cos\mu)][Z''_-(\sigma_-)-Z''_+(x_s\sin\mu-h\cos\mu)]\}dx_s. \quad (5.13)$$

5.1. *The functions $Z''_+(\sigma_+)$ and $Z''_-(\sigma_-)$*

It follows from (5.9) and (2.7) that, when Z''_+ is real and positive,

$$\frac{\sigma_+}{2h\cos\mu} = \frac{1}{\pi}\{Z''^{\frac{1}{2}}_+ - \tan^{-1}Z''^{\frac{1}{2}}_+\}, \quad (5.14)$$

where $Z''^{\frac{1}{2}}_+$ is real and positive. Thus, in $\sigma_+ > 0$, Z''_+ is a real-valued monotonic function, and its values are given in figure 7. When σ_+ is small,

$$Z''_+ \doteq \left\{\frac{3\pi\sigma_+}{2h\cos\mu}\right\}^{\frac{2}{3}}, \quad (5.15)$$

and, when the line $\sigma_+ = 0$ is crossed from $\sigma_+ > 0$ to $\sigma_+ < 0$, amp σ_+ increases by π (Hurley 1969). Hence, when σ_+ is a small negative quantity amp $Z''_+ = 2\pi/3$. It follows from (5.9) that, when σ_+ is real negative, Z''_+ is the complex-valued function defined by

$$Z'' = r\exp\{i\theta\}, \quad 2\pi/3 < \theta < 4\pi/3, \quad (5.16)$$

where
$$r = -1 + 2r^{\frac{1}{2}}\sin\theta/2\left\{\frac{1+\exp\{-4r^{\frac{1}{2}}\sin\theta/2\}}{1-\exp\{-4r^{\frac{1}{2}}\sin\theta/2\}}\right\}, \quad (5.17)$$

and
$$\frac{\sigma_+}{2h\cos\mu} = \frac{1}{\pi}\left\{r^{\frac{1}{2}}\cos\theta/2 - \tfrac{1}{2}\tan^{-1}\frac{2r^{\frac{1}{2}}\cos\theta/2}{1-r}\right\}. \quad (5.18)$$

Also,
$$Z''^{\frac{1}{2}}_+ = r^{\frac{1}{2}}\exp\{i\theta/2\}. \quad (5.19)$$

Numerical values are shown in figures 7 and 8. When σ_+ is negative, Z''_+ is a periodic function with period $2h\cos\mu$, and, as σ_+ is decreased by this amount, the contour Γ shown in figure 8 is described once in the positive sense.

To discuss Z''_- we need to consider separately the three regions into which the physical plane is divided by its boundaries and the line $\sigma_- = 0$. These are shown in figure 9.

In region I, σ_- is negative and Z''_- is the real, positive monotonic function defined by

$$\frac{\sigma_-}{-2h\cos\mu} = \frac{1}{\pi}\{Z''^{\frac{1}{2}}_- - \tan^{-1}Z''^{\frac{1}{2}}_-\}, \quad (5.20)$$

where $Z''^{\frac{1}{2}}_-$ is real and positive.

Equations (5.14) and (5.20) show that the value of $Z''_-(\sigma_-)$ for points in region I are given by
$$Z''_-(-s) = Z''_+(s) \quad (s > 0). \quad (5.21)$$

Also,
$$Z''^{\frac{1}{2}}_-(-s) = Z''^{\frac{1}{2}}_+(s) \quad (s > 0). \quad (5.22)$$

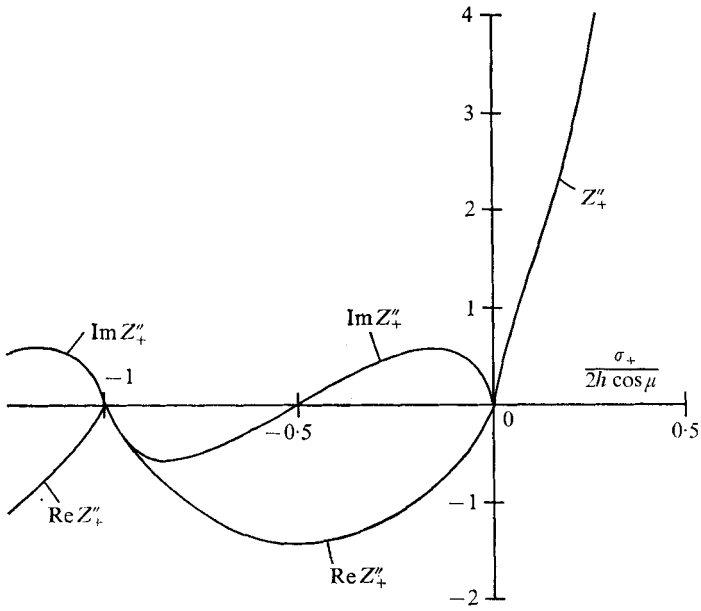

FIGURE 7. Values of function $Z''_+(\sigma_+)$.

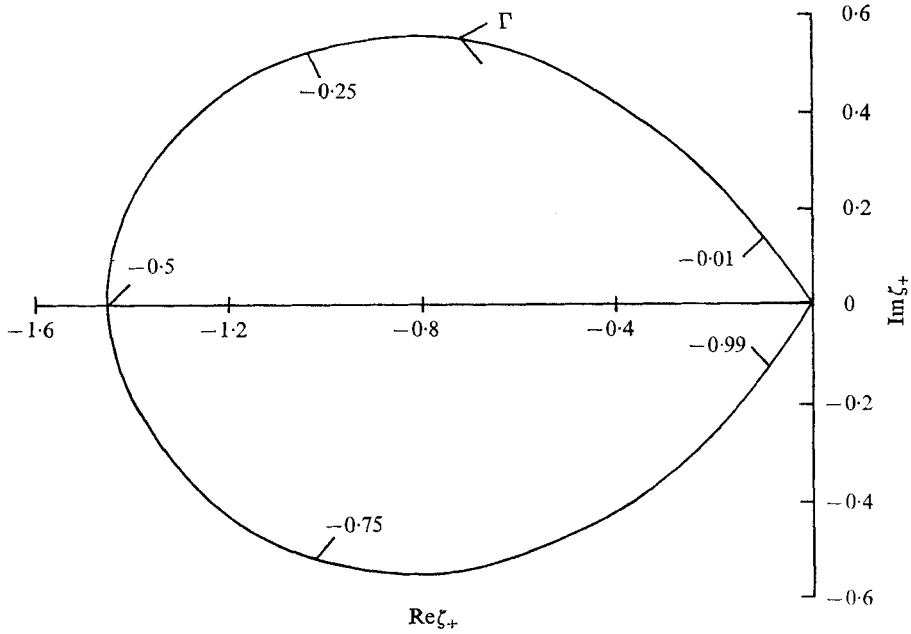

FIGURE 8. Argand diagram of the function $\zeta_+[\sigma_+/(2h\cos\mu)] = Z''_+(\sigma_+)$. Numbers on curve denote values of $\sigma_+/(2h\cos\mu)$.

By examining the behaviour of $Z''_-(\sigma_-)$ near its branch points, we may determine its values throughout regions II and III of figure 9, and establish the following relations. For points in regions II and III,

$$Z''_-(s+2h\cos\mu) = Z''_+(s) \qquad (-\infty < s < \infty), \tag{5.23}$$

and

$$Z''^{\frac{1}{2}}_-(s+2h\cos\mu) = -Z''^{\frac{1}{2}}_+(s) \quad (-\infty < s < \infty). \tag{5.24}$$

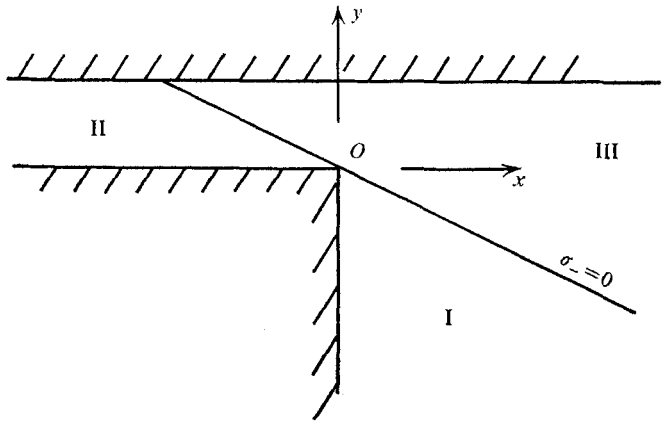

FIGURE 9. Definition of regions I, II and III.

5.2. *Simplification of the solution* (5.12) *and* (5.13)

Each of the terms in (5.12) and (5.13) has branch points for certain values of σ_+ and σ_-. The appropriate indentations around them may be found by the method given in § 2. Also, various terms in each equation may be combined, and, making use of (5.21) and (5.23), we find that

$$\begin{aligned}\psi'_+(\sigma_+) = {} & \frac{U}{2\pi}\int_0^\infty \exp\{ikt\}\log[Z''_+(\sigma_+) - Z''_+(t)]\,dt \\ & + \frac{U}{2\pi}\int_{-2h\cos\mu}^0 \exp\{-ik(t+2h\cos\mu)\}\log[Z''_+(\sigma_+) - Z''_+(t)]\,dt \\ & + \frac{U}{2\pi}\int_0^\infty \exp\{-ik(t+2h\cos\mu)\}\log[Z''_+(\sigma_+) - Z''_+(t)]\,dt, \qquad (5.25)\end{aligned}$$

and

$$\begin{aligned}\psi'_-(\sigma_-) = {} & -\frac{U}{k}\exp\{-ik\sigma_-\}H_{\mathrm{II}}(-\sigma_-) \\ & - \frac{U}{2\pi}\int_0^\infty \exp\{ikt\}\log[Z''_-(\sigma_-) - Z''_+(t)]\,dt \\ & - \frac{U}{2\pi}\int_{-2h\cos\mu}^0 \exp\{-ik(t+2h\cos\mu)\}\log[Z''_-(\sigma_-) - Z''_+(t)]\,dt \\ & - \frac{U}{2\pi}\int_0^\infty \exp\{-ik(t+2h\cos\mu)\}\log[Z''_-(\sigma_-) - Z''_+(t)]\,dt, \qquad (5.26)\end{aligned}$$

where $H_{\mathrm{II}}(-\sigma_-)$ in the first term of (5.26) denotes the Heaviside step function, the subscript II having been added to denote that it is non-zero only for σ_- negative and in region II of figure 9. Details of the integration paths for the various terms in (5.25) and (5.26) are given in table 1.

Let
$$\zeta_+\left(\frac{\sigma_+}{2h\cos\mu}\right) = Z''_+(\sigma_+) \qquad (5.27)$$

and
$$\zeta_-\left(\frac{\sigma_-}{2h\cos\mu}\right) = Z''_-(\sigma_-). \qquad (5.28)$$

Term	Branch point(s) of integrand	Sense of indentation
1st in (5.25)	σ_+ if $\sigma_+ > 0$	Below
2nd in (5.25)	$\sigma_+ + 2Mh\cos\mu$ if $\sigma_+ < 0$ (See caption)	Above
3rd in (5.25)	σ_+ if $\sigma_+ > 0$	Above
2nd in (5.26)	σ_- if $\sigma_- < 0$ and σ_- in region I of figure 9 $2h\cos\mu - \sigma_-$ if $\sigma_- > 0$	Below Above
3rd in (5.26)	σ_- of $2Nh\cos\mu$ if $\sigma_- < 2h\cos\mu$ and σ_- not in region I of figure 9 (See caption)	Below if $0 < \sigma_- < 2h\cos\mu$ Above if $\sigma_- < 0$
4th in (5.26)	σ_- if $\sigma_- > 0$ $2h\cos\mu - \sigma_-$ if σ_- in region I of figure 9	Below Above

TABLE 1. Indentations for the integration paths in (5.25) and (5.26). M is the non-negative integer such that $-2h\cos\mu < \sigma_+ + 2Mh\cos\mu < 0$ when $\sigma_+ < 0$, and N is the non-negative integer such that $0 < \sigma_- + 2Nh\cos\mu < 2h\cos\mu$ when $\sigma_- < 2h\cos\mu$.

Then, from (5.9) and (5.10),

$$\frac{d\zeta_+}{d\sigma_+} = 2\pi\frac{1+\zeta_+}{\zeta_+^{\frac{1}{2}}}, \quad \frac{d\zeta_-}{d\sigma_-} = -2\pi\frac{1+\zeta_-}{\zeta_-^{\frac{1}{2}}}, \tag{5.29}$$

and differentiation of (5.25) gives

$$\frac{d\psi'_+}{d\sigma_+} = \frac{U(1+\zeta_+)}{\zeta_+^{\frac{1}{2}}}\left\{\int_0^\infty \frac{\exp\{iks\}ds}{\zeta_+(\sigma'_+)-\zeta_+(s)} + \int_{-1}^0 \frac{\exp\{-ik(s+1)\}}{\zeta_+(\sigma'_+)-\zeta_+(s)}ds + \int_0^\infty \frac{\exp\{-ik(s+1)\}}{\zeta_+(\sigma'_+)-\zeta_+(s)}ds\right\}, \tag{5.30}$$

where

$$\sigma'_+ = \sigma_+/(2h\cos\mu), \tag{5.31}$$

and

$$K = 2kh\cos\mu. \tag{5.32}$$

The integrals in (5.30) are transformed as follows. The integration path for the first term is displaced to the positive imaginary axis, and the integration path for the third term to the negative imaginary axis. In the second term the variable of integration is changed to $\zeta_+(s)$, so that the integration path becomes the closed contour Γ (shown in figure 8) but is described in the negative sense. This path is then displaced to the interval $(-1, 0)$ of the real axis described twice. These transformations in conjunction with a similar treatment of (5.26) lead to the following equation for the fluid velocity V:

$$\begin{aligned} V = {} & \text{Reflected waves} \\ & + \frac{U\hat{\sigma}_+(1+\zeta_+(\sigma'_+))}{\zeta_+^{\frac{1}{2}}(\sigma'_+)}\left\{i\int_0^\infty \frac{\exp\{-K\tau\}d\tau}{\zeta_+(\sigma'_+)-\zeta_+(i\tau)} - i\exp\{-iK\}\int_0^\infty \frac{\exp\{-K\tau\}d\tau}{\zeta_+(\sigma'_+)-\zeta_+(-i\tau)}\right. \\ & \left. + \frac{i}{\pi}(\exp\{-iK\}-1)\int_0^1 \exp\{K\tau/\pi\}\left(\frac{1-\tau}{1+\tau}\right)^{K/2\pi}\frac{\tau^2 d\tau}{(1-\tau^2)(\zeta_+(\sigma'_+)+\tau^2)}\right\} \\ & + \frac{U\hat{\sigma}_-(1+\zeta_-(\sigma'_-))}{\zeta_-^{\frac{1}{2}}(\sigma'_-)}\left\{i\int_0^\infty \frac{\exp\{-K\tau\}d\tau}{\zeta_-(\sigma')-\zeta_+(i\tau)} - i\exp\{-iK\}\int_0^\infty \frac{\exp\{-K\tau\}d\tau}{\zeta_-(\sigma'_-)-\zeta_+(-i\tau)}\right. \\ & \left. + \frac{i}{\pi}(\exp\{-iK\}-1)\int_0^1 \exp\{K\tau/\pi\}\left(\frac{1-\tau}{1+\tau}\right)^{K/2\pi}\frac{\tau^2 d\tau}{(1-\tau^2)(\zeta_-(\sigma'_-)+\tau^2)}\right\}. \end{aligned} \tag{5.33}$$

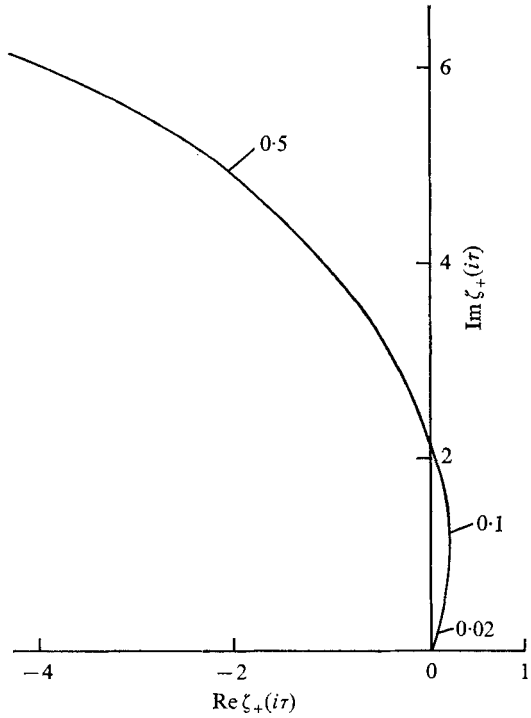

FIGURE 10. Trace of the function $\zeta_+(i\tau)$ in the Argand diagram. The numbers on the curve denote values of τ.

Here $\hat{\sigma}_+$ and $\hat{\sigma}_-$ are unit vectors in the directions $\exp\{i\mu\}$ and $\exp\{i(\pi-\mu)\}$ respectively and the reflected waves are those that are obtained using the laws of reflexion for infinite plane surfaces (Phillips 1966, p. 176). Also,

$$\sigma'_- = \sigma_-/(2h\cos\mu), \tag{5.34}$$

and $\zeta_+(i\tau)$ and $\zeta_+(-i\tau)$ are the analytic continuations of the function ζ_+ defined by (5.27) onto the positive and negative imaginary axes, respectively. $\zeta_+(-i\tau)$ is the complex conjugate of $\zeta_+(i\tau)$, whose trace in the Argand diagram is shown in figure 10.

5.3. *Discussion of solution*

Equation (5.33) gives the fluid velocity as the sum of the reflected and the diffracted waves. Since the former gives zero normal velocity on the boundaries, so too should the latter. The form of (5.33) in conjunction with (5.21) to (5.24) shows that this is in fact the case.

We now show that our solution satisfies the radiation condition in the shadow zone above the continental shelf. The stream function ψ for the total motion is given by (5.2), (5.11), (5.25) and (5.26). The first term of (5.26) cancels ψ_i in the shadow zone, and it follows from these equations, §5.1 and table 1 that in this zone ψ must be of the form $F(\sigma_+)-F(\sigma_-)$ for some F. Also, here $Z''_-(\sigma_-)$ and $Z''_+(\sigma_+)$ are periodic functions with period $2h\cos\mu$, so that

$$\psi = \sum_{n=-\infty}^{\infty}{}' C_n\left\{\exp\left\{\frac{-in\pi\sigma_+}{h\cos\mu}\right\}-\exp\left\{\frac{-in\pi\sigma_-}{h\cos\mu}\right\}\right\}, \tag{5.35}$$

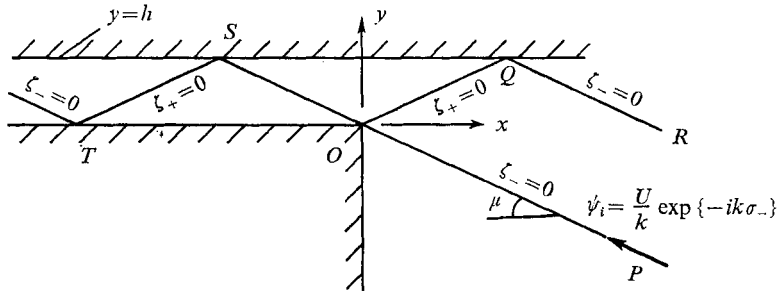

FIGURE 11. The lines in the physical plane on which ζ_+ or ζ_- vanish, and near which the velocities in the diffracted waves are significant when $K = 2kh\cos\mu$ is large.

where
$$C_n = \frac{1}{2h\cos\mu}\int_0^{2h\cos\mu} \psi'_+(\sigma_+)\exp\left\{\frac{in\pi\sigma_+}{h\cos\mu}\right\}d\sigma_+. \tag{5.36}$$

Using (5.9) and (5.31), (5.36) can be written as

$$C_n = \frac{U}{2\pi}\oint_\Gamma \left(\frac{1-i\zeta_+^{\frac{1}{2}}}{1+i\zeta_+^{\frac{1}{2}}}\right)^n \exp\{2in\zeta_+^{\frac{1}{2}}\}\frac{\zeta_+^{\frac{1}{2}}}{1+\zeta_+}\psi'_+\,d\zeta_+, \tag{5.37}$$

where Γ is the contour shown in figure 8, indented in such a way that the branch points at $\zeta_+ = 0$ and $Z''_+ = Z''_+(t)$ (see (5.25)) lie outside it. In this expression, $\zeta_+^{\frac{1}{2}} = i$ at $\zeta_+ = -1$, so that the integrand has a pole of order $n+1$ at this point when n is positive, and is regular there when n is negative. Thus

$$C_n = 0, \quad n < 0, \tag{5.38}$$

so that
$$\psi = \sum_{n=1}^{\infty} C_n\left\{\exp\left\{\frac{-in\pi\sigma_+}{h\cos\mu}\right\} - \exp\left\{\frac{-in\pi\sigma_-}{h\cos\mu}\right\}\right\}; \tag{5.39}$$

and the C_n may be calculated from (5.37) using the calculus of residues. Equation (5.39) expresses ψ as the sum of waves moving to the left, so that the Sommerfeld radiation condition is satisfied in the region above the continental shelf.

When K is large, the major contributions to the integrals in (5.33) are obtained from small values of τ, so that, by (5.15) and (5.31), the approximations

$$\zeta_+(i\tau) = (3\pi\tau)^{\frac{2}{3}}\exp\{i\pi/3\} \quad \text{and} \quad \zeta_+(-i\tau) = (3\pi\tau)^{\frac{2}{3}}\exp\{-i\pi/3\}$$

may be used therein. It is then apparent that the velocities in the diffracted waves will be significant only near the lines on which either ζ_+ or ζ_- vanishes. These are shown in figure 11, and are (as expected) the edges of the reflected waves. Also, if we express the velocities in the diffracted waves in the form

$$UV_{+D}(\sigma'_+)\,\hat{\sigma}_+ + UV_{-D}(\sigma'_-)\,\hat{\sigma}_-, \tag{5.40}$$

then near the line $\sigma_- = 0$ we find that

$$V_{-D}(\sigma_-) \doteqdot \frac{+i\hat{\sigma}_-}{3\pi(-\sigma'_-)^{\frac{1}{3}}}\left\{\int_0^\infty \frac{\exp\{-K\tau\}\,d\tau}{(-\sigma'_-)^{\frac{2}{3}} - \tau^{\frac{2}{3}}\exp\{i\pi/3\}} - \int_0^\infty \frac{\exp\{-K\tau\}\,d\tau}{(-\sigma'_-)^{\frac{2}{3}} + \tau^{\frac{2}{3}}}\right.$$
$$\left. + \exp\{-iK\}\left[-\int_0^\infty \frac{\exp\{-K\tau\}\,d\tau}{(-\sigma'_-)^{\frac{2}{3}} - \tau^{\frac{2}{3}}\exp\{-i\pi/3\}} + \int_0^\infty \frac{\exp\{-K\tau\}\,d\tau}{(-\sigma'_-)^{\frac{2}{3}} + \tau^{\frac{2}{3}}}\right]\right\}. \tag{5.41}$$

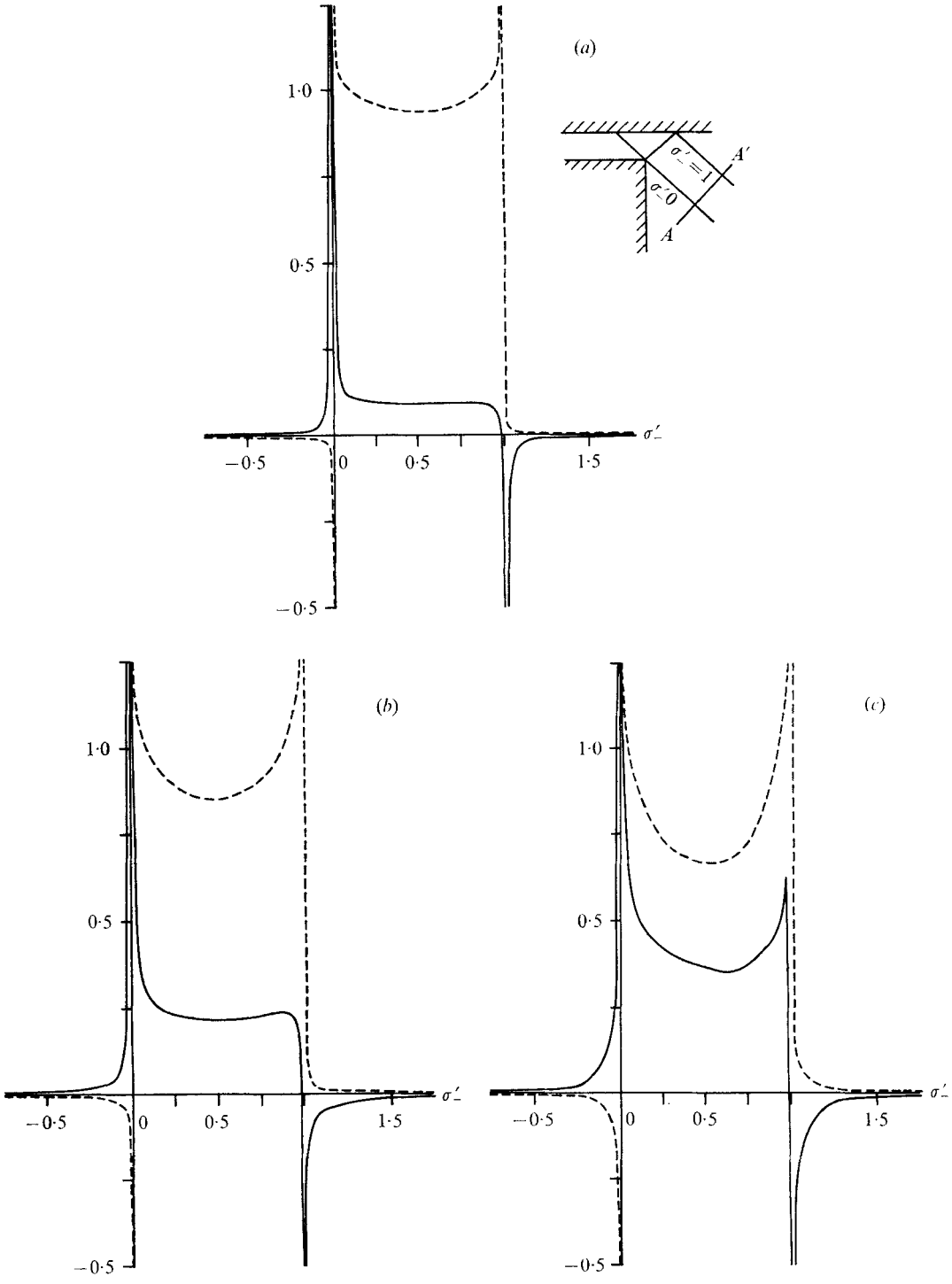

FIGURE 12. For legend see facing page.

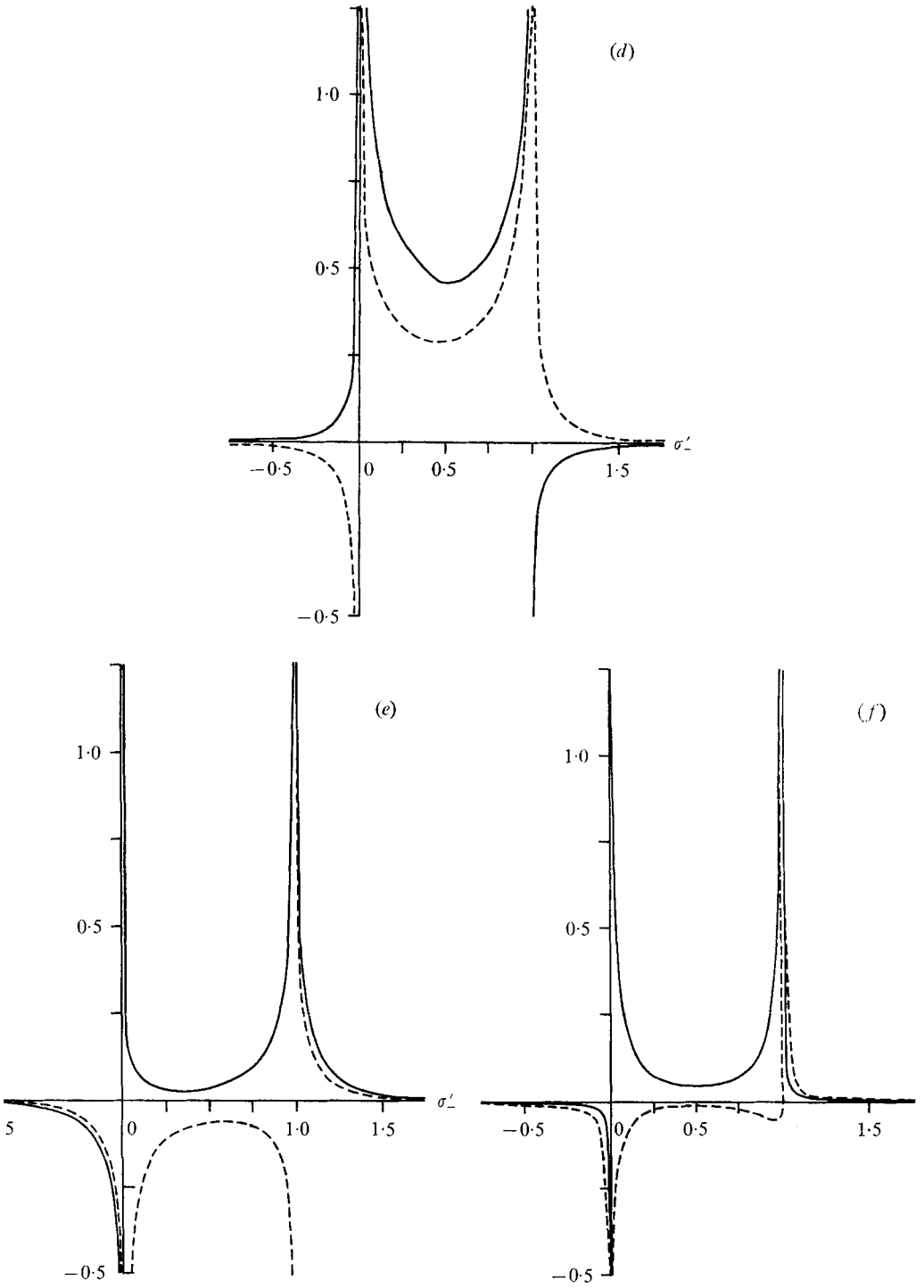

FIGURE 12. Values of the diffracted velocity V_{-D} at various points on a line such as AA' shown in the insert. ———, $\mathrm{Re}\,V_{-D}$; – – – –, $\mathrm{Im}\,V_{-D}$. K: (*a*) 0·2, (*b*) 0·5, (*c*) 1·0, (*d*) 2·0, (*e*) 5·0, (*f*) 10·0.

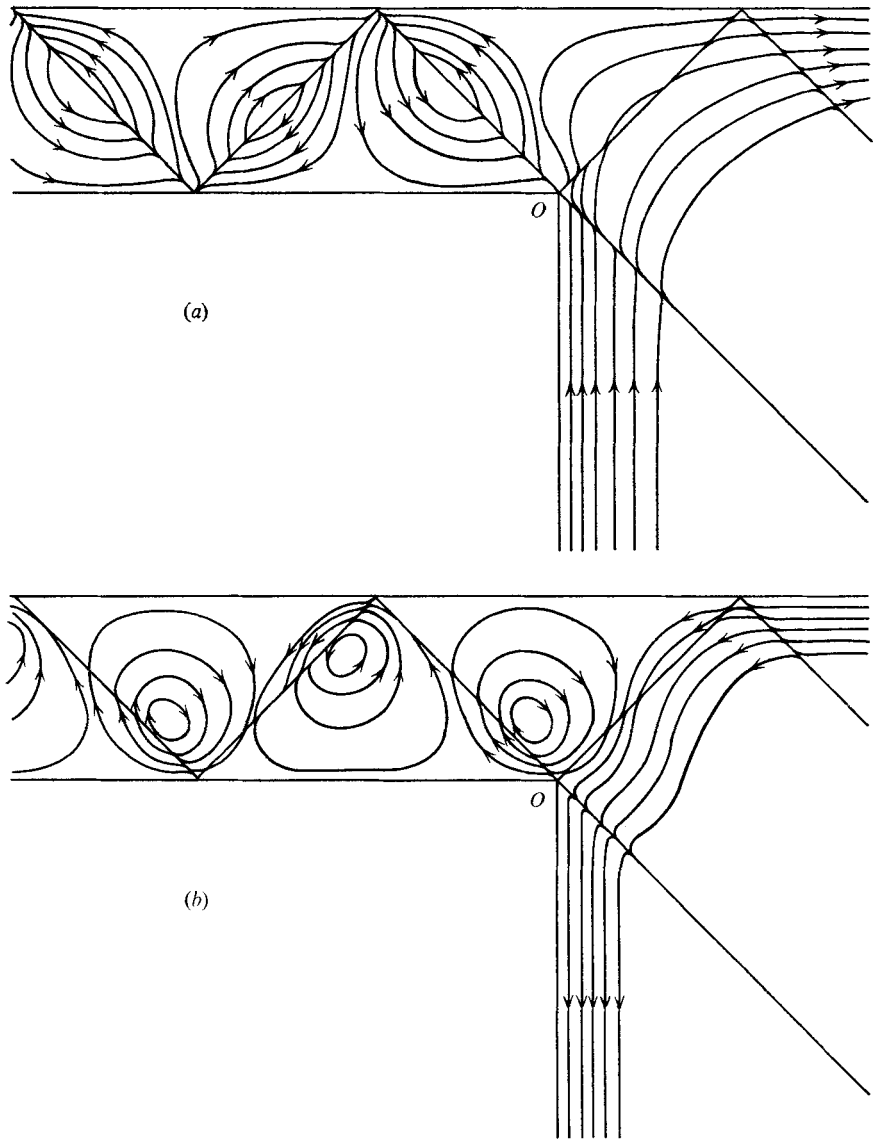

FIGURE 13. Instantaneous streamlines for $K = 1$. (*a*) Lines on which the real part of ψ is constant. (*b*) Lines on which the imaginary part of ψ is constant.

Referring to Hurley (1970), we see that the first and second terms in (5.41) give the diffracted waves that occur when the wave ψ_i is incident on the corner at O in the absence of the boundary at $y = h$, and that the third and fourth terms give the diffracted waves that would occur if the wave reflected from the boundary $y = h$ were incident on the corner at O in the absence of the boundary at $y = h$.

Figure 12 gives values of V_{-D} for various values of K (defined by (5.32)) for points on a line such as AA' shown in the insert of figure 12(*a*). When K is large, V_{-D} is significant only when σ'_- is nearly zero or unity (figure 12(*f*)). As K is decreased, the regions in which V_{-D} is significant increase, and for K less than

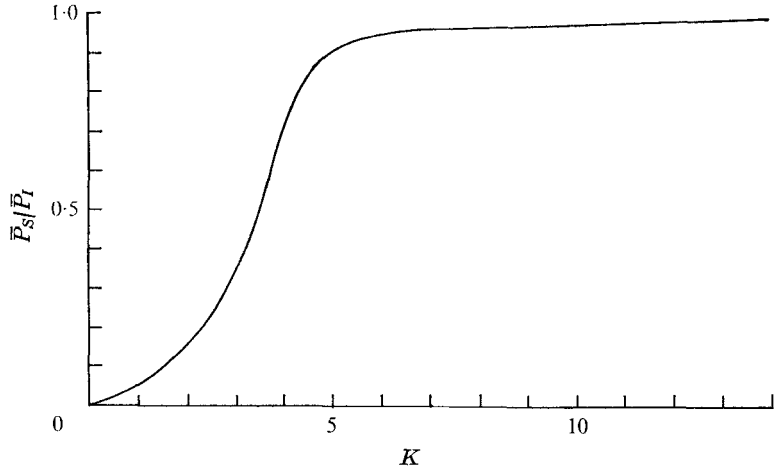

FIGURE 14. Energy flux above continental shelf.

about two it is significant throughout $0 < \sigma'_- < 1$. In the limit $K \to 0$ it may be shown analytically that

$$V_{-D} \to i, \quad 0 < \sigma'_- < 1,$$
$$\to 0, \quad \sigma'_- < 0, \quad \sigma'_- > 1. \tag{5.42}$$

This behaviour is apparent in the results for $K = 0{\cdot}2$ (figure 12(*a*)). It is interesting to note that the velocities given in (5.42) are minus the corresponding limiting velocities in the incident plus reflected waves. Hence, in the limit $K \to 0$, the total fluid velocity tends to zero.

The instantaneous streamlines for the case $K = 1$ are shown in figure 13. The fluid velocity is infinite along each of the characteristics that pass through the corner O, and this leads to their being tangential to these characteristics either with a point of inflexion or with a cusp there, depending on whether or not the fluid velocity changes direction as the characteristic is crossed (see also figure 12). The most noticeable feature in the region above the continental shelf is the cellular nature of the instantaneous streamlines. Of course, our solution, which is based on the linearized equations of motion, is invalid near the characteristics on which it is singular, but it seems unlikely that this local breakdown will influence greatly the main features of the flow (Robinson 1970*b*).

By using the method of Hurley (1970) it may be shown that the ratio of the mean energy flux (in the horizontal direction) above the continental shelf $\bar{P}_S$ to the mean energy flux $\bar{P}_I$ in the incident wave between $\sigma'_- = 0$ and $\sigma'_- = 1$ is

$$\frac{\bar{P}_S}{\bar{P}_I} = 1 + \int_0^\infty \{K[uv^{(-1)} - u^{(-1)}v + u^{(-1)}\cos K\sigma'_- - v^{(-1)}\sin K\sigma'_-] - u\sin K\sigma'_- - v\cos K\sigma'_-\}d\sigma'_-, \tag{5.43}$$

where $V_{-D} = u + iv$,

$$u^{(-1)} = \int_0^{\sigma'_-} u\,d\sigma'_- \quad \text{and} \quad v^{(-1)} = \int_0^{\sigma'_-} v\,d\sigma'_-. \tag{5.44}$$

Numerical values are given in figure 14. When K is large, the diffracted waves are unimportant, and all the incident energy is transmitted above the shelf. As K decreases, the fraction that is transmitted decreases monotonically to zero.

The author is grateful to Mr M. E. Fisher for carrying out the numerical analysis and computer programming needed to prepare figures 12–14, and to the Australian Research Grants Committee for financial support.

REFERENCES

BAINES, P. G. 1971*a* The reflexion of intenal/inertial waves from bumpy surfaces. *J. Fluid Mech.* **46**, 273.

BAINES, P. G. 1971*b* The reflexion of internal/inertial waves from bumpy surfaces. Part 2. Split reflexion and diffraction. *J. Fluid Mech.* **49**, 113.

BARCILON, V. & BLEISTEIN, N. 1969*a* Scattering of inertial waves in a rotating fluid. *Studies in Appl. Math.* **48**, 91.

BARCILON, V. & BLEISTEIN, N. 1969*b* Scattering of inertial waves by smooth convex cylinders. *Studies in Appl. Math.* **48**, 351.

BERS, L., JOHN, F. & SCHECHTER, M. 1964 *Partial Differential Equations.* Interscience.

CARRIER, G. F., KROOK, M. & PEARSON, C. E. 1966 *Functions of a Complex Variable.* McGraw-Hill.

HURLEY, D. G. 1969 The emission of internal waves by vibrating cylinders. *J. Fluid Mech.* **36**, 657.

HURLEY, D. G. 1970 Internal waves in a wedge-shaped region. *J. Fluid Mech.* **43**, 97.

LIGHTHILL, M. J. 1966 On waves generated in dispersive systems by travelling forcing effects, with applications to the dynamics of rotating fluids. *J. Fluid Mech.* **27**, 725.

MILNE-THOMSON, L. M. 1949 *Theoretical Hydrodynamics* (2nd edn.). Macmillan.

PHILLIPS, O. M. 1966 *The Dynamics of the Upper Ocean.* Cambridge University Press.

ROBINSON, R. M. 1970*a* The effects of a corner on a propagating internal gravity wave *J. Fluid Mech.* **42**, 257.

ROBINSON, R. M. 1970*b* Ph.D. thesis, University of Western Australia.